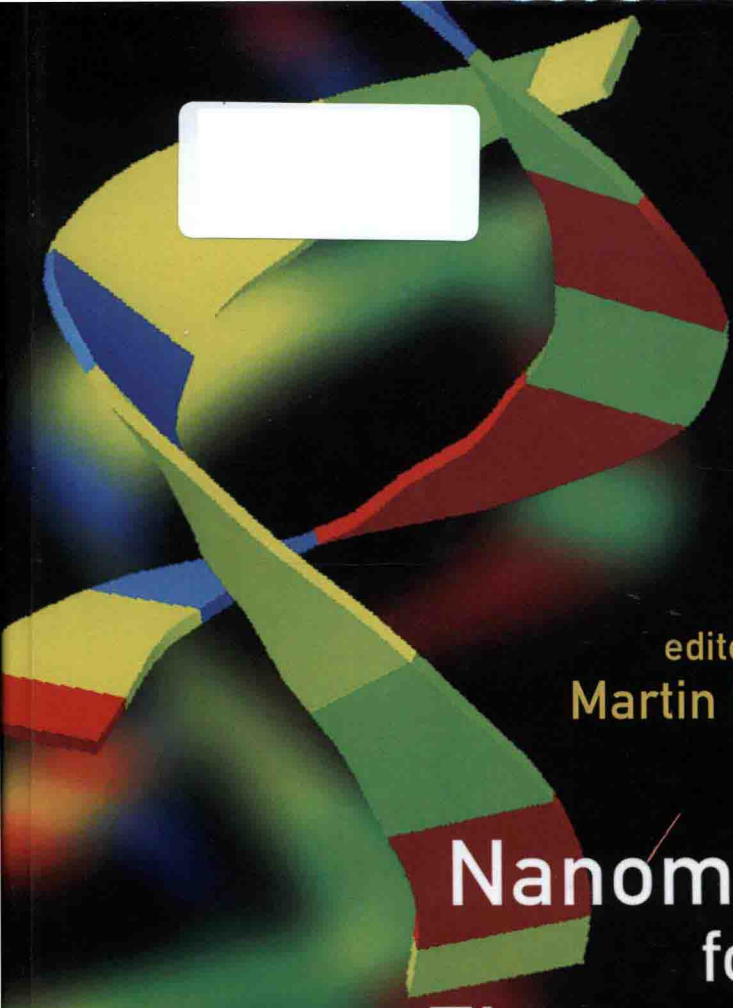

edited by
Martin Pumera

Nanomaterials for Electrochemical Sensing and Biosensing

Nanomaterials for Electrochemical Sensing and Biosensing

edited by
Martin Pumera

Pan Stanford Publishing

Published by

Pan Stanford Publishing Pte. Ltd.
Penthouse Level, Suntec Tower 3
8 Temasek Boulevard
Singapore 038988

Email: editorial@panstanford.com
Web: www.panstanford.com

British Library Cataloguing-in-Publication Data
A catalogue record for this book is available from the British Library.

ISBN 978-981-4364-90-4 (Hardcover)
ISBN 978-981-4364-91-1 (eBook)

Printed in the USA

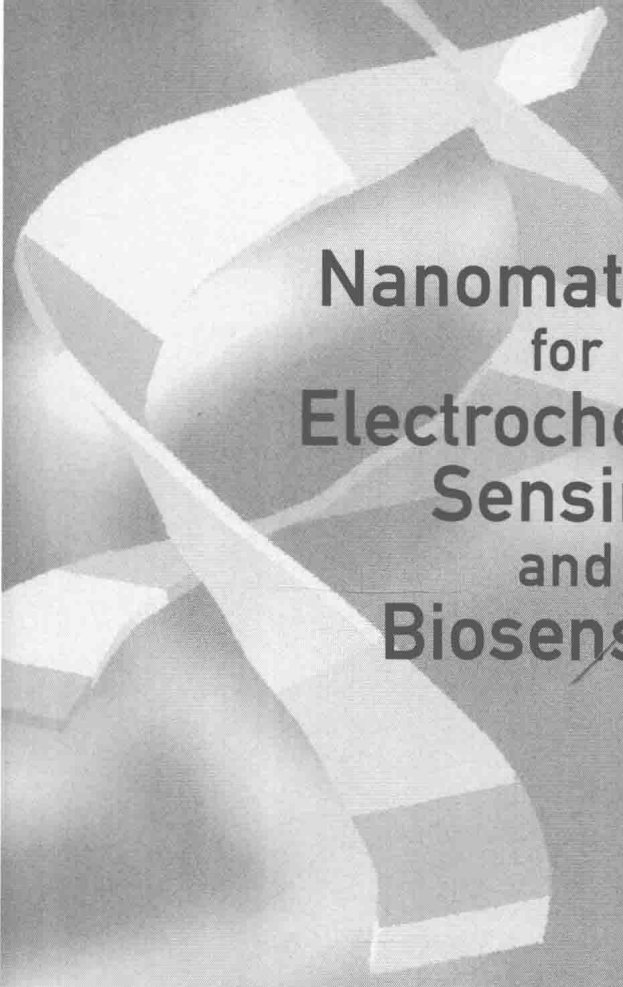

Nanomaterials for Electrochemical Sensing and Biosensing

Preface

This book reviews the important achievements in the field of nanomaterial-based electrochemical sensors and biosensors. Nanotechnology brings new possibilities for the development of sensors, biosensors, and electrochemical bioassays. Nanoscale materials have been extensively used in a wide variety of configurations: as electrode surfaces to promote electrochemical reaction, as "wires" to enzymes connecting their redox centers to electrode surface, as nanobarcodes for biomolecules, and as tags to amplify the signal of a biorecognition event. Nanomaterial-based electrochemical sensors have been used in many areas, including cancer diagnostics and the detection of infectious organisms.

It is my pleasure to present an excellent overview of this area from established and active research scientists in this dynamic field. The book consists of seven chapters, each describing different aspects of electrochemical sensing and biosensing. It aims to provide a comprehensive overview of this crucial field.

Martin Pumera
March 2014
Singapore

Contents

Chapter 1

Nanomaterials for Electrochemical Sensing and Biosensing

Jonathan P. Metters and Craig E. Banks
Faculty of Science and Engineering, Manchester Metropolitan University, Chester Street, Manchester M1 5GD, Lancs, UK
c.banks@mmu.ac.uk

In this chapter we explore the voltammetric responses that can be observed at regular and random arrays and how characterization via voltammetry may be sought. We also briefly consider the voltammetry at nanoparticle-modified electrodes and provide an overview of the various regular and random arrays that have been developed and utilized in electrochemical sensing, such as metallic, boron-doped diamond, screen-printed, and carbon nanotube arrays.

1.1 Introduction

The pioneering work of Wightman and Fleishman on microelectrodes has undoubtedly significantly advanced the field of electrochemistry [1]. The International Union of Pure and Applied Chemistry (IUPAC) conventionally assumes that a microelectrode

Nanomaterials for Electrochemical Sensing and Biosensing
Edited by Martin Pumera

ISBN 978-981-4364-90-4 (Hardcover), 978-981-4364-91-1 (eBook)
www.panstanford.com

has a dimension of tens of micrometers or less, down to the submicrometer range [1]. Microelectrodes have the inherent advantage of a reduced ohmic drop, the rapid establishment of a steady-state signal output, an increased signal-to-noise ratio, and a current increase due to enhanced mass transport [1–10]. While these improvements are highly beneficial and allow electrochemical reaction mechanisms and kinetics to be determined, trace electrochemical analysis to be achieved, and in vivo measurements to be applied, and also apply to highly resistive media, the very low current output is highly undesirable. This problem can be simply overcome through the application of a *microelectrode array*.

Let us consider the voltammetry at an array of microelectrodes, as depicted in Fig. 1.1, where the dark circles in the scheme represent the microelectrodes that are at a fixed distance from their nearest neighbors in a cubic geometry [11].

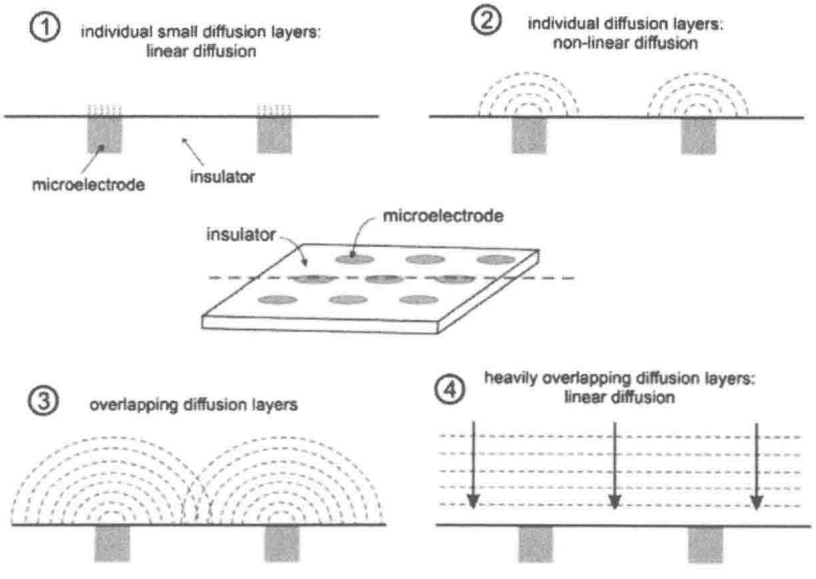

Figure 1.1 Schematic diagram of the four categories a diffusion profile may belong to an array of microelectrodes (reproduced from Ref. [11] with permission from Elsevier).

If we consider the simple electrochemical case of a one-electron redox couple, *A*, undergoing electrolysis to a product, *B*, as the applied potential is increased and the onset of electrolysis results in the oxidation of *A* to *B*, a depletion layer grows around each of

the microdiscs. The voltammetry at a microelectrode array can be divided into four intuitive categories [11], where it can be readily observed that the magnitude of the diffusional zone against that of the microelectrode size, as well as the separation between the microelectrodes on the array, is critical.

In category 1, the diffusional layer, as represented by the dashed lines in Fig. 1.1, is small in magnitude compared to the geometric size of the microdisc, which results in the dominating mass transport to be that of planar diffusion, where the voltammetric response is similar to that observed at a macroelectrode. In category 2, as is evident in Fig. 1.1, the diffusion layers are larger than that of the microelectrodes, but it is important to note they do not interact with neighboring diffusion domains. This regime, where radial diffusion is the dominant form of mass transport, is the ideal response that all electrochemists desire. The response at a simple microelectrode is given by

$$I_{\mathrm{LIM}} = nFrDC \tag{1.1}$$

where a sigmoidal limiting current, I_{LIM}, will be observed due to radial diffusion. In the case of a microelectrode array, as depicted in Fig. 1.1, the current response at the array, I_{array}, is given by

$$I_{\mathrm{array}} = 4nFrCDN \tag{1.2}$$

where now the current response is multiplied by N, the total number of microelectrodes comprising the array. Thus the response on an array, if operating in this category 2 Fig. 1.1 Image B, clearly allows the amplification of the analytical signal. This is particularly important as identified above, where one can harness the advantages of a microelectrode and overcome the limitations of small (nA) signals that would otherwise be engulfed in electrical noise. Amplification at the analytical signal will allow for enhanced sensing levels with high sensitivities and low levels of analytes to be confidently measured, and hence advantageous limits of detection may be realized. To determine that one is in this region, scan rate–independent voltammetry will be observed where the current is proportional to the radius of the microelectrodes comprising the array. Table 1.1 depicts the typical characteristics that are associated with these four categories (Fig. 1.1).

As is evident in Fig. 1.1, category 3 is also a possibility for microelectrode arrays, where, in this case, diffusional interaction occurs such that a purely sigmoidal voltammetric response has a

slight-to-clear peak shape depending on the severity of the diffusional overlap where scan rate dependence will be readily observed. In this regime, the microelectrodes adjacent to each other deplete the same region of the solution, leading to a decrease in the magnitude of the voltammetric peak height in comparison to that observed in category 2. The last category (category 4) is where the diffusional zones heavily overlap and planar diffusion is the dominant form of mass transport. The current response here is dependent upon the square root of the scan rate in accordance with that of a macroelectrode governed by the Randles–Ševćik equation (see Table 1.1).

Table 1.1 Linear sweep and cyclic voltammetry characteristics associated with the four categories presented in Fig. 1.1, where δ is the size of the diffusion zone, r is the microdisc radius, d is the center-to-center separation, I_P is the peak current, I_{LIM} is the limiting current, and v is the scan rate (reproduced from Ref. [11] with permission from Elsevier)

	Category			
Property	**1**	**2**	**3**	**4**
δ **vs.** r	$\delta < r$	$\delta > r$	$\delta > r$	$\delta > r$
δ **vs.** d	$\delta < d$	$\delta < d$	$\delta > d$	$\delta > d$
Type of response	Clear peak $\rightarrow I_P$	Steady state $\rightarrow I_{LIM}$	Slight peak to clear peak $\rightarrow I_P$	Slight peak to clear peak $\rightarrow I_P$
Scan rate dependence	Yes	No	Yes	Yes
Current dependence	$I_P \propto v^{0.5}$	$I_{LIM} \propto r$	–	$I_P \propto v^{0.5}$

In addition to the above insights, Guo and Lindner [12] built upon these providing guidelines for the design of coplanar and recessed microdisc arrays. Figure 1.2 depicts simulated concentration profiles and the corresponding observed voltammetric responses, along with an elegant zone diagram, as depicted in Fig. 1.3, allowing researchers to clearly identify and characterize the response of their microelectrode array. The dimensionless scan rate, V (used in Fig. 1.3), is given by

$$V = \frac{nF}{4RT}\frac{\upsilon r^2}{D} \tag{1.3}$$

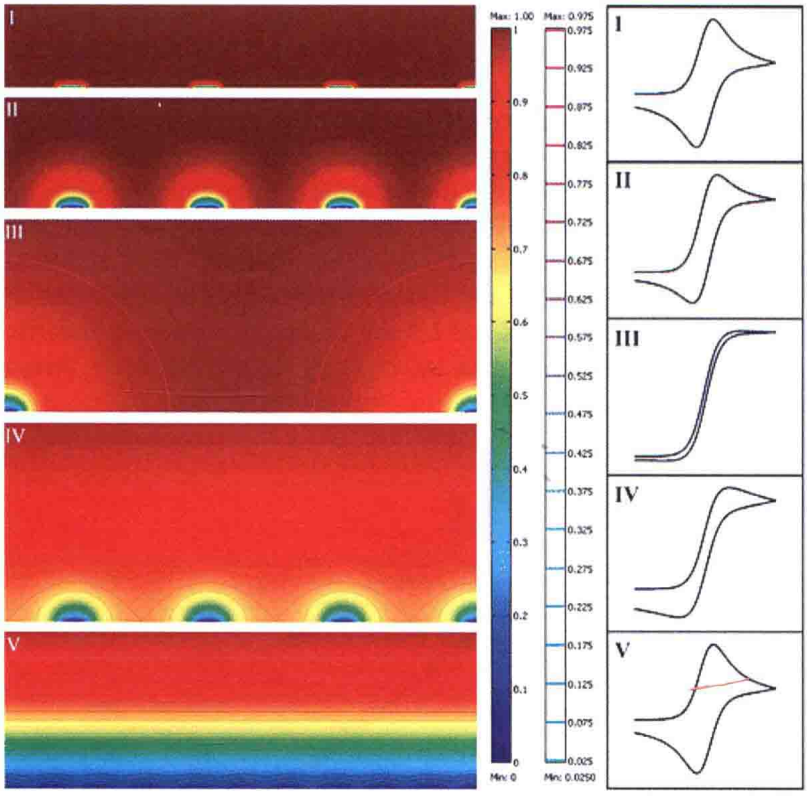

Figure 1.2 Simulated concentration profiles with isoconcentration contour lines over a microelectrode array representing the five main categories of diffusion modes: (1) planar diffusion layers on individual microdiscs, (2) mixed diffusion layers on microdiscs (diffusion mode between planar and hemispherical diffusion), (3) hemispherical diffusion layers on individual microdiscs, (4) mixed diffusion layers (diffusion mode of partial overlapping of adjacent diffusion layers), and (5) planar diffusion layers over the entire microelectrode array (diffusion mode of complete overlapping of individual diffusion layers). In the scale bar next to the figure, the red color represents the bulk concentration and the blue color represents zero concentration. The second scale bar represents a relative concentration scale for the contour lines. Typical *CV*s of each category are shown at the right. Note, this is for the case of a hexagonal arranged array. (Reproduced from Ref. [12], copyright 2005, American Chemical Society.)

where, r is the radius of an individual electrode comprising the array and υ is the applied voltammetric scan rate, with all other symbols

having their usual meaning. The zone diagram (Fig. 1.3) is highly informative as it allows one to deduce which diffusional region the array under investigation is in and how experimental parameters via the dimensionless scan rate, V (see Eq. 1.3), can readily change the diffusional regime and hence dramatically change the voltammetric response [12]. Note that the dimensionless transition scan rates in Fig. 1.3, depicted as $V12$, $V23$, $V34$, and $V45$, represent the borderlines between the diffusions modes I, II, II, and III; III and IV (II and IV in certain domains); and IV and V, respectively (all as per the notation in Fig. 1.2). Using Figs. 1.2 and 1.3 one may predict the voltammetric response of one's array and intelligently design electrode arrays [11].

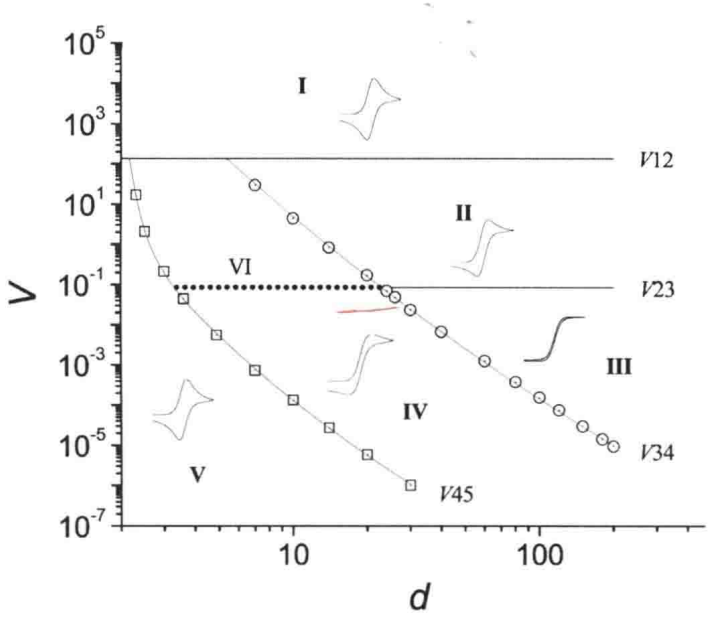

Figure 1.3 Zone diagram of cyclic voltammetric behavior at microelectrode arrays. d is the center-to-center distance of individual electrodes in the array (measured in units of r), V is the dimensionless scan rate (see Eq. 1.3). Note, this is for a hexagonal arrangement. (Reproduced from Ref. [12], copyright 2005, American Chemical Society.)

Additionally Guo and Lindner have considered the case of shallow recessed microdisc arrays, since, typically, lithography and other fabrication methods produce these types of electrodes rather than the usually assumed true planar arrays. An elegant equation